

# A Nonlinear Model for Transient Responses from Light-Adapted Wolf Spider Eyes

ROBERT D. DEVOE

From the Department of Physiology, The Johns Hopkins University School of Medicine,  
Baltimore, Maryland 21205

**ABSTRACT** A quantitative model is proposed to test the hypothesis that the dynamics of nonlinearities in retinal action potentials from light-adapted wolf spider eyes may be due to delayed asymmetries in responses of the visual cells. For purposes of calculation, these delayed asymmetries are generated in an analogue by a time-variant resistance. It is first shown that for small incremental stimuli, the linear behavior of such a resistance describes peaking and low frequency phase lead in frequency responses of the eye to sinusoidal modulations of background illumination. It also describes the overshoots in linear step responses. It is next shown that the analogue accounts for nonlinear transient and short term DC responses to large positive and negative step stimuli and for the variations in these responses with changes in degree of light adaptation. Finally, a physiological model is proposed in which the delayed asymmetries in response are attributed to delayed rectification by the visual cell membrane. In this model, cascaded chemical reactions may serve to transduce visual stimuli into membrane resistance changes.

In the previous paper (DeVoe, 1967), there were described some of the properties of nonlinear step responses from light-adapted wolf spider eyes. It was shown that transients in these responses were of two types. Short-term transient responses were over in about one-half sec, while long-term transients or "creep" lasted 15 sec or more, by which time steady-state DC responses were reached. The purpose of the present paper is to develop a quantitative model for the short-term transients in nonlinear step responses. This model will be a quantitative embodiment of the qualitative schema developed in the previous paper to explain the waveforms of short term responses. A preliminary presentation of a different variation of the model has been presented elsewhere (DeVoe, 1966).

The bases for the model were presented in the previous paper (DeVoe, 1967) and will be summarized as follows: First, nonlinearities in short-term step responses do not develop instantaneously; they are delayed in time. These delays are assumed to explain why there are peak responses which overshoot

the asymmetrical (i.e., nonlinear) short-term DC responses to positive and negative incremental step stimuli. It is also assumed that the overshoots in linear responses to small incremental steps (DeVoe, 1963) are due to the same delay process. The dynamics of overshoot in linear step responses can be quantitated from the frequency responses of the spider eye (DeVoe, 1963, 1964). Therefore, these dynamics ought to represent the incremental, linearized behavior of the process responsible for delayed nonlinearities in responses to large incremental steps. This is the crux of the present model.

As will be shown subsequently, the overshooting or peaking in linear step and frequency responses, respectively, of the spider eye can be duplicated by an electrical analogue containing inductance, capacitance, and resistance (Fig. 3). So too can the small signal, incremental behavior of a biased, thermonegative, time-variant resistance (Ekelöf and Kihlberg, 1954; Mauro, 1961). The nonlinear behavior of the current-biased (directly heated), thermonegative time-variant resistance to large incremental current steps is, moreover, like the simple delayed asymmetries schema presented in the previous paper (DeVoe, 1967). (Since such a resistance cannot change instantaneously because its temperature cannot change instantaneously, directly heating it by an incremental current step causes the initial voltage drop to be in proportion to the current whereas the final voltage drop is not.) Finally, there is much resemblance between the responses of such a time-variant resistance and those of biological and artificial membranes to electrical stimuli (Mauro, 1961). Thus, the delays in asymmetries in spider eye responses might be due to the dynamics of its receptor cell membranes, as for example delayed rectification by these membranes. This possibility has been uppermost in mind while developing the present model and will be returned to at the end of this paper.

The second consideration for the model is the latent period of response. Fuortes and Hodgkin (1964) have analyzed the relation of latency and rate of rise to sensitivity in intracellular responses from *Limulus* ommatidia. A portion of their paper is devoted to small amplitude, linear responses to small flashes and steps of light. There, they found that the responses of an analogue composed of  $n$ , identical exponential delay sections reproduced the waveforms of the linear ommatidial responses. Exposure to light was assumed to reduce the time constants in all but one section of the analogue, thus relating observed decreases in latency, peak response time, and sensitivity. The point of this linear analysis was that decreases in time constant would directly decrease speed of response, but would decrease sensitivity by the  $n-2$ th power (where  $n$  was the total number of sections in the "dark-adapted" analogue).

In spider eyes too there are large changes in sensitivity with changes in degree of adaptation, whereas there are but small simultaneous changes in time course of response (DeVoe, 1967). Likewise,  $n$  exponential delays will account for the steep high frequency attenuations observed in frequency

responses of spider eyes (DeVoe, 1963, 1964), in flies' eyes (Kuiper and Leutscher-Hazelhoff, 1965), and in human flicker vision (deLange, 1961). In these frequency analyses, it has sufficed for the time constants of the exponential delays to be taken as constant over the frequency ranges of interest (0.5 to  $>100$  cps). In the present model, a similar assumption will be made. The latent period of the spider eye responses, and the high frequency falloff in flicker responses of this eye will be represented in the model by a chain of identical exponential delays. The time constant of these exponential delays, although different at different steady states of light adaptation, will be assumed to vary (due to a changed background illumination) with a time course slow in comparison with one-half sec or 0.5 cps. The present model, then, is composed of two serial stages, one containing exponential delays with time constants which are constant (at least during a short-term response) and one containing time-variant resistance.

Others have also developed models of nonlinear transient responses. Jones, Green, and Pinter (1962) proposed that autocatalytic chemical kinetics might explain observed time courses of *Limulus* generator potentials. The nonlinearities were introduced in part by this autocatalysis, in part by a logarithmic scaling of the stimulus. The origins of the logarithmic scaling were not identified. Troelstra (1964) proposed that a time-dependent, nonlinear scaler operated upon the stimulus to determine its efficacy in eliciting the human scotopic retinal action potential. Finally, Fuortes and Hodgkin (1964), in the latter part of their paper, argued that the nonlinearities in potentials elicited by strong light from dark-adapted *Limulus* ommatidia could be due to parametric feedback of these potentials upon the shunt conductances (and hence the time constants) of their exponential delay analogue. This RC feedback model does attempt to account for those short-term nonlinearities in responses of dark-adapted *Limulus* eyes which are the results of "rapid desensitization." It does not, on the other hand, account for the slow effects of light adaptation upon the time constants of their analogue. However, Rushton (1965) proposed that "dark light" from bleached photopigments could also feed back parametrically upon these time constants, at least in the human eye. Marimont (1965) obtained an improved fit of the RC feedback model to dark-adapted *Limulus* eye responses when the feedback voltage was taken from the next-to-last exponential delay section of the model. Lastly, Pinter (1966) sought to reproduce with the RC feedback model the shapes of the frequency responses of light-adapted *Limulus* ommatidia. Parameters in the model which gave only a fair fit to the recorded frequency responses gave an even worse fit to measured step responses of dark-adapted ommatidia. As it stands, therefore, the RC feedback model appears to be unable to encompass short-term responses of both light-adapted and dark-adapted eyes.

From the above, it can be seen that there is an essential difference between

the present model for responses of light-adapted spider eyes and the RC feedback model (Fuortes and Hodgkin, 1964) for responses of dark-adapted *Limulus* eyes. In the present model, the time constants of exponential delay are assumed to remain constant over the first half-sec of response and hence to contribute nothing to the observed nonlinearities. In the RC feedback model, variation in these time constants is the source of the nonlinearities in response during the first half-sec. Since the two models describe two different states of adaptation, it is possible that there is less conflict between them than appears. This will be taken up again at the end of this paper.

On the other hand, the RC feedback model alone appears unable to account for the responses of light-adapted wolf spider eyes. For one thing, it predicts no phase lead at all in frequency responses (Pinter, 1966), whereas in the spider eye there may be phase lead of up to  $+45^\circ$  in responses to sinusoidal modulations of background illumination (DeVoe, 1964). Second, the time constants of exponential delay in the spider eye as determined from frequency responses (DeVoe, 1964) are already so small (on the order of 2–3 msec) that further reduction in these time constants by feedback during an incremental step could not lead to the half-sec long nonlinear transients observed (DeVoe, 1967). For these reasons and those given at the beginning of this paper, the model to be presented below was developed.

#### EXPERIMENTAL METHODS

The preparation of wolf spiders for recording retinal action potentials was essentially as described in the preceding paper (DeVoe, 1967). However, in some early experiments with linear responses, the indifferent electrode was placed upon the posterior lateral eye contralateral to the illuminated posterior median eye; this posterior lateral eye was shielded from stray light by a small piece of black paper waxed to the animal (DeVoe, 1963). There appeared to be no quantitative differences between linear responses recorded using this eye as an indifferent electrode and linear responses recorded using an indifferent electrode placed posteriorly on the animal's carapace.

The results to be presented here were obtained using only the previously described glow modulator tube source (DeVoe, 1967). This source provided a constant background illumination which could be changed not only in steps, but sinusoidally as well. Sinusoidal voltages were obtained from a Krohn-Hite 440-A oscillator (Krohn-Hite Corp., Cambridge, Mass.), and their amplitudes were measured with a Ballantine 316 infrasonic peak-to-peak voltmeter (Ballantine Laboratories, Inc., Boonton, N. J.). The amplitudes of these sinusoidal voltages used to drive the light source were attenuated as desired with the same attenuator used to vary the amplitudes of step voltage inputs to the light source.

Responses to steps and flashes were analyzed as described in the preceding paper (DeVoe, 1967). Two methods were used to analyze the responses to sinusoidal stimulation. Initially, one vertical amplifier of a Tektronix 502 oscilloscope was made into a tuned amplifier by connecting a Muirhead D-925-B tunable twin-t filter (Muirhead Instruments, Inc., Mountainside, N. J.) in a feedback loop between its output

and its input. The  $Q$  of this tuned amplifier could be varied from 25 to 250 (feedback ratios of 0.01 to 0.1, respectively) depending upon the signal to noise improvement needed and upon the frequency. (It was not practical to use a high  $Q$  at low frequencies, as it took too long for the amplifier to settle down.) The amplifier was tuned by adjusting the filter to have minimum output at the driving frequency. This tuned amplifier was useful in separating small ( $1-2 \mu\text{v}$ ) sinusoidal responses from the noise ( $15 \mu\text{v}$  or more) in the recording preamplifier, but it was very sensitive to DC drifts in the preparation when it was tuned to frequencies less than 5 cps. At these low frequencies a measurement of the amplitude of response often took up to a half hour. Tuned amplification for frequencies below 40 cps was therefore discarded when signal averaging with the LINC computer was begun. For stimuli above 40 cps, the responses were often so small that a Tektronix 122 AC preamplifier modified to give 10 or 100 times gain was used in series with the gain of 20 DC preamplifier. The additional noise contributed by this AC preamplifier was sufficiently great that the responses had to be filtered with the tuned amplifier before they could be averaged by the computer.

For off-line averaging of responses to sinusoidal stimuli with the LINC computer, the stimulus and responses waveforms were both recorded on an FM analogue tape recorder along with analysis gate waveforms lasting one cycle each. Recording and playback speeds as well as computer sampling rates were adjusted so that the computer sampled each stimulus and response waveform at about 200 points whenever the analysis gate was present. The number of responses averaged varied between 128 and 512. An example of the averaged responses and stimuli, as photographed on the computer oscilloscope, is shown in Fig. 1 a. At the end of each of these waveforms are a few extraneous points which presumably are there because of analysis gate jitter. These points are best seen in the modified display in Fig. 1 b; from such a display they could be eliminated point by point until a smooth sinusoid was judged by eye to remain. The amplitude of this sinusoid was measured by moving a displayed line under manual control until it coincided with the peaks, as in Fig. 1 c. The difference between the peaks was stored as the amplitude (in arbitrary units), and the position halfway between the peaks was taken as the base line. This base line was then displayed, as in Fig. 1 d, along with a vertical line which could be moved under manual control until it coincided with the zero crossings. The zero crossings of both response and stimulus waveforms were then used to compute the phase, which was displayed along with the amplitude, as shown in Fig. 1 e. Amplitudes and phase of sinusoidal responses found this way agreed well, within experimental error, with those determined by Fourier analysis of the averaged responses (see below).

Transfer functions were fitted by eye to amplitude and phase plots (such as those in Fig. 4 below) with the aid of a Boonshaft and Fuchs frequency response slide rule; this slide rule was especially helpful in finding quadratic poles. Calculations of the step responses of the fitted transfer functions and calculations based on non-linear differential equations were performed on IBM 1401 and 7094 computers.

In five experiments, the points representing the averaged sinusoidal stimuli and responses were punched, via paper tape, onto cards and a Fourier analysis was performed on both with the 7094 computer to determine the harmonics and the phase

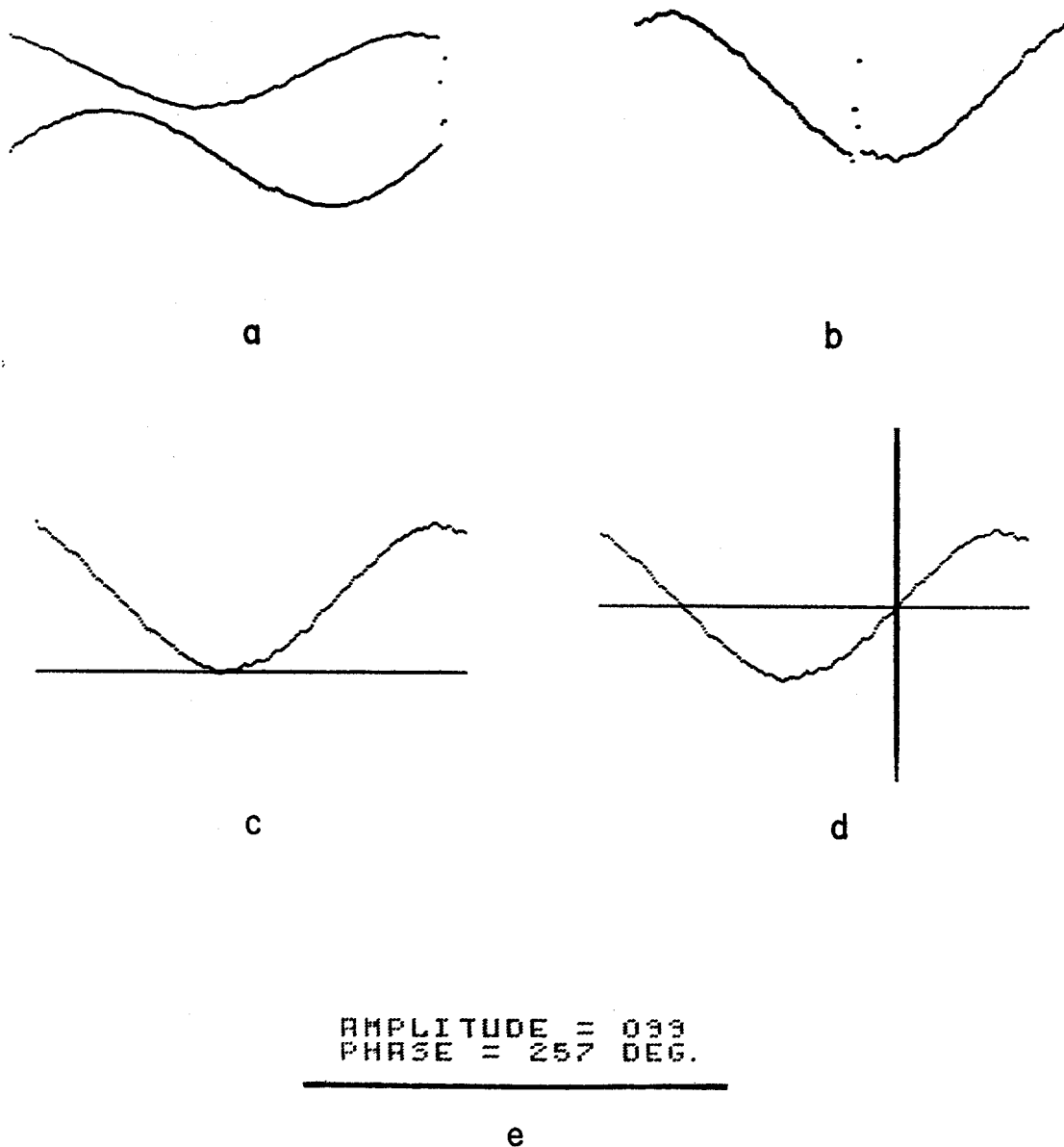


FIGURE 1. Determination of response amplitudes and phases with the LINC computer. The photographs are of displays on the computer oscilloscope of points making up the averaged waveforms of stimuli and responses. (a) Averaged response (upper trace) and averaged stimulus (lower trace); each trace is made up of about 200 points. (b) The averaged response has been rotated in phase; that is, it has been shifted along the x-axis, with the beginning of the original display now following the end of the original display. The obviously out-of-place points can be eliminated one-by-one to yield a smooth sinusoid. (c) A horizontal line generated by the computer is moved in the display under potentiometer control until it coincides by eye with the peak(s) of the sine wave. (d) The computer

between them. The results from one experiment are shown in Table I. There is a good match between the amplitudes and phases measured using the LINC computer and the amplitudes and phases of the fundamentals of the sets of points representing the averaged responses. The LINC estimations of amplitudes are almost always a bit

TABLE I  
PEAK-TO-PEAK MICROVOLTS OF RESPONSE, AND PHASE OF  
RESPONSE RELATIVE TO PHASE OF STIMULUS, DETERMINED FROM  
AVERAGED RESPONSES USING THE LINC COMPUTER  
AND BY PERFORMING FOURIER ANALYSES  
UPON THE AVERAGED RESPONSES

Cycles per second	Peak-to-peak microvolts response		Phase of response, in degrees	
	From LINC	From Fourier fundamental	From LINC	From Fourier fundamental
1.00	10.0	9.7	+27	+24
1.26	10.4	10.1	+18	+18
1.59	10.0	9.7	+18	+16
2.00	9.3	9.1	+17	+16
2.52	9.6	9.3	+8	+8
3.18	7.8	7.8	-2	+4
4.00	15.2	14.9	-18	-18
5.03	11.1	10.8	-34	-34
6.34	8.2	8.4	-55	-56
7.98	10.4	10.4	-79	-79
10.0	18.5	18.3	-97	-98
12.6	25.6	25.4	-124	-124
15.9	24.5	24.4	-151	-152
20.0	24.5	24.5	-181	-185
25.2	20.8	20.3	-217	-219
31.8	20.0	19.5	-258	-260
40.0	21.5	21.1	-304	-307
44.9	20.4	20.0	-332	-333
50.3	21.5	21.3	-363	-364
56.5	19.7	19.5	-389	-389
63.4	14.8	14.6	-423	-427
71.1	8.0	8.9	-454	-453
79.8	5.2	5.2	-489	-488

larger than the amplitudes of the fundamentals, but in Table I, this was never by more than  $2\frac{1}{2}\%$  except at 71 cps, and then the amplitude was underestimated on the LINC. Evaluation of the harmonics of these responses showed that the 2nd harmonic did not exceed 5% of the fundamental and was usually less, while the 3rd

displays a horizontal base line midway between the peaks (determined as in (c)) and a vertical line which is moved along the x-axis under potentiometer control to coincide by eye with the zero crossings. (e) The amplitude is displayed as the difference (in relative units) between the peaks of the sine wave response. The displayed phase of the response relative to the stimulus is computed from the zero crossings of the averaged stimulus and response waveforms, as in (d), and from the number of points set as in (b).

harmonic did not exceed 3%. Thus the responses averaged were primarily sinusoids, signifying that the spider eye was responding linearly (DeVoe, 1963).

It has been found by others that at low frequencies, the responses to large amplitude sinusoidal stimuli are distorted, whereas at high frequencies they are not (Kirschfeld, 1961; Kuiper and Leutscher-Hazelhoff, 1965; Pinter, 1966). Such distortion also appears in responses of wolf spider eyes to large amplitude sinusoidal stimuli of less than 3 cps. The Fourier analyses of such responses to several am-

TABLE II  
HARMONIC CONTENTS OF AVERAGED RESPONSES TO VARIOUS  
AMPLITUDES OF SINUSOIDAL STIMULI IN THE RANGE 0.798 TO 5.03  
CPS, AS DETERMINED BY FOURIER  
ANALYSES OF THESE AVERAGED RESPONSES  
For comparison, amplitudes and phases of averaged responses as determined  
with the LINC and from the Fourier fundamental are shown.

Cycles per second	Peak-to-peak microvolts response		Harmonics as per cents of fundamental		Phase of response, in degrees	
	From LINC	From fundamental	2nd	3rd	From LINC	From fundamental
0.798	8.3	7.9	3.03	0.43	+45	+42
	17.5	16.3	14.5	1.06	+39	+39
	31.1	29.1	22.1	4.11	+31	+35
1.26	8.3	7.9	15.9	7.44	+34	+36
	14.6	14.0	7.2	1.21	+39	+33
	28.8	26.4	20.1	1.0	+34	+31
2.00	9.9	9.5	7.05	3.15	+22	+20
	24.8	24.3	11.15	0.41	+27	+25
	42.0	40.1	16.9	2.11	+28	+25
3.18	11.6	10.6	4.79	1.21	0	+3
	27.1	27.3	4.23	0.30	0	+6
	40.7	40.2	6.19	0.89	0	-1
5.03	11.9	12.1	1.59	1.20	-33	-34
	27.8	27.6	1.53	0.81	-31	-34
	44.6	44.3	1.55	1.03	-30	-31

plitudes of stimuli in the range of 0.8 to 5.0 cps, are shown in Table II. There, it can be seen that increasing the size of the responses increases the amount of 2nd and 3rd harmonics in them, and that this increase in harmonic content is for the most part only evident below 3 cps. It also appears that even with a rich harmonic content, the amplitudes and phases of averaged responses are about the same whether determined with the LINC or from the Fourier fundamental. In practice, harmonic distortions at low frequency were avoided by recording only responses of about 10  $\mu$ v peak-to-peak.



## T H E O R Y

*A Nonlinear Analogue for the Spider Eye* An electrical analogue which will duplicate the behavior of the light-adapted spider eye is shown in Fig. 2. It consists of two sections, one made up of  $n$  cascaded exponential delay stages which provide the latency of response, and one nonlinear stage containing a time-variant resistance  $R_T$  shunted by a capacitance  $C_T$ . The isolating transconductances  $g$  are a mathematical convenience and permit changes in the value of  $R_T$  to be directly reflected in changes in  $V$ , the response of the analogue. It is now supposed that  $R_T$  responds like a thermonegative, time-variant resistance, such that for an increase in  $i_T$  (due to an increase in input  $I$  to the analogue),  $R_T$  slowly decreases to a new value due to the increased

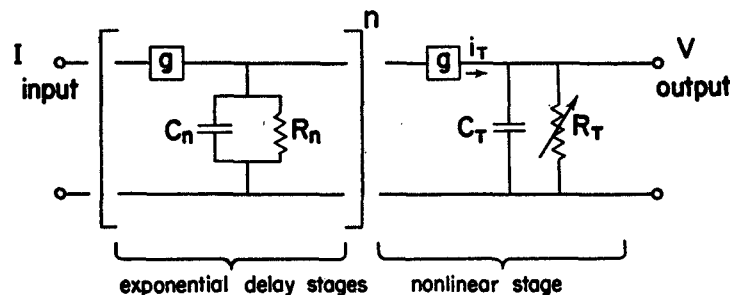


FIGURE 2. An analogue of nonlinear and linear responses from light-adapted wolf spider eyes. The input  $I$  to the analogue is the sum of the background illumination  $I_0$  and positive or negative changes  $\Delta I$  in this background. The output  $V$  of the analogue is taken to be the recorded retinal action potentials and is the sum of the background potential  $V_0$  (the response to  $I_0$ ) and the incremental responses  $\Delta V$  to changes in the background illumination. See text for details.

voltage across it, while for a decreased  $i_T$ , it slowly increases to a new value. In other words,  $R_T$ , and hence the voltage developed across it, displays delayed nonlinearities. With this analogue, therefore, the applicability of delayed nonlinearities to description of light-adapted spider eye responses can be tested.

Two further points about the choice of this particular analogue must be made. First, as stated above, the exponential delay stages are assumed to have constant time constants for the first half-sec after strong incremental stimulation. In addition to the reasons given above, there is the possibility that creep, or long term transients in step responses (DeVoe, 1967), might be explained by very slow changes in exponential delay time constants. This will be taken up in a qualitative way at the end of this paper. Since creep becomes evident only about one-half sec following a step stimulus, little violence is done by assuming that the exponential delay time constants don't change during a

short-term response. In addition, it makes the calculations simpler because it is then possible to treat the exponential delay stages as linear over the duration of short-term responses.

Second, it is assumed that the nonlinear stage in the analogue follows the exponential delay stages. This is because this nonlinear stage may be best thought of as representing behavior of the visual cell membranes, as will be brought out in the discussion later. It is also because it doesn't make much difference in what order the two sections of the analogue come. Because, as will be shown, the time constant of the time-variant resistance stage is so much larger than those of exponential delay, the calculated responses of both orderings are almost identical. The theoretical behavior of the analogue with the nonlinear stage preceding the exponential delays has been presented elsewhere (DeVoe, 1966).

#### Definition

- $I_o$  = ambient background illumination upon the eye
- $\Delta I$  = positive or negative step change in  $I_o$
- $I = I_o + \Delta I$
- $V_o$  = background potential, the steady-state DC response to  $I_o$
- $\Delta V$  = positive or negative response superimposed upon  $V_o$
- $V = V_o + \Delta V$
- $(v_i)_o, \Delta v_i, v_i$  = responses of the  $i$ th exponential delay stage
- $\tau_e = R_n C_n$ , the time constant of the exponential delay stages, assumed to be all the same
- $\tau_T = R_T C_T$ , the instantaneous time constant of the nonlinear stage with  $C_T$  assumed to remain constant
- $A = \left(\frac{g}{C_n}\right)^n \frac{g}{C_T}$ , the scaling factor which is assumed to be constant and independent of degree of light adaptation.

*Nonlinear Step Responses* To begin with, the short-term responses of the exponential delay stages are analyzed as though they were linear. (For details, see the linear analysis of such stages by Fuortes and Hodgkin, 1964.) The behavior of any one exponential delay stage is given by

$$\frac{dv_i}{dt} = \frac{g}{C_n} v_{i-1} - \frac{v_i}{\tau_e} \quad (1)$$

To a step  $\Delta I$  applied to the input of the analogue, the incremental response of the  $n$ th or final exponential delay stage is given by

$$\Delta v_n = \Delta I \left(\frac{g}{C_n}\right)^n \tau_e^n \left[ 1 - e^{-\frac{t}{\tau_e}} \sum_{r=0}^{n-1} \left(\frac{t}{\tau_e}\right)^r / r! \right] \quad (2)$$

The steady-state response  $(v_n)_o$  to a constant background illumination  $I_o$  is seen from equation (2) to be

$$(v_n)_o = I_o \left( \frac{g}{C_n} \right)^n \tau_e^n$$

The response  $V$  of the nonlinear stage, which is taken to be the recorded retinal action potential, is related to  $v_n$  as follows:—

$$C_T \frac{dV}{dt} + \frac{V}{R_T} = g \cdot v_n$$

For an incremental response  $\Delta V$ , and rearranging the above,

$$\frac{d\Delta V}{dt} + \frac{\Delta V}{\tau_T} = \left( \frac{g}{C_T} \right) \Delta v_n \quad (3)$$

Writing  $S(t)$  for the quantity in brackets in equation (2) and recalling the definition of  $A$ , the response of the analogue to a step  $\Delta I$  superimposed upon  $I_o$  is given by addition of the above:

$$\frac{dV}{dt} + \frac{V}{\tau_T} = [I_o + \Delta I \cdot S(t)] A \tau_e^n \quad (4)$$

$\tau_T$  may be determined using the steady-state solution of equation (4)

$$\tau_T = \frac{V}{IA\tau_e^n} \quad (5)$$

Hence at steady state the two time constants are interrelated.

The essence of delayed nonlinearities is that after a current step across it,  $R_T$  (and hence  $\tau_T$ ) changes slowly, but not instantaneously. This could occur, for example, if  $R_T$  was dependent upon another variable which, in the simplest case, was described by a first order equation. For a thermonegative time-variant resistance, the other variable is the power  $P$  dissipated by  $R_T$ . Two equations describe such a resistance (see Appendix I); in the context of the analogue, these equations are

$$\tau_T = c_1 \exp \left[ \frac{c_2}{P/c_3 + 1} \right] \quad (6)$$

$$T \frac{dP}{dt} + P = \frac{V^2}{\tau_T} \quad (7)$$

(Ekelöf and Kihlberg, 1954). Briefly,  $R_T$  depends on  $P$  as determined by equation (6); this is the result of it being a thermonegative resistance. The dissi-

pated power  $P$  can only change at a rate determined by the thermal time constant  $T$  and the amount of supplied power  $V_2/\tau_T$ . No physiological meaning is to be attached to this "dissipated power" (Mauro, 1961) or to the other parameters, however, since only a formal analogy is being made here to permit subsequent computation of visual responses.

When all transients in response have died away, equation (7) reduces to

$$P = \frac{V^2}{\tau_T} \quad (8)$$

This may be combined with equation (5) to give

$$P = V \cdot I \cdot A \tau_e^n \quad (9)$$

$P$  at steady state may therefore be determined solely as a function of  $V$  and  $I$ .

A further simplification is made by differentiating equation (6):

$$\frac{d\tau_T}{dt} = -\tau_T \left( \frac{c_2}{c_3} \right) \left( \frac{1}{P/c_3 + 1} \right)^2 \frac{dP}{dt} \quad (10)$$

The parameter  $c_1$  is thus eliminated.  $C_2$  is essentially independent of state of light adaptation, but  $c_3$  (and  $c_1$ ) is not (see Appendix II).

*Dependence of Analogue Parameters upon Degree of Light Adaptation* The less light-adapted wolf spider eye is more sensitive but has slower response time courses. It also has a lower background potential due to the lower background illumination but has short-term DC responses to given per cent changes in background illumination which are simply scaled down in proportion to the reduced background potential (DeVoe, 1967). These observations may be incorporated into the nonlinear analogue by supposing that at each different, lower background illumination, increased time constants  $\tau_e$  and  $\tau_T$  (corresponding to increased shunt resistances  $R_n$  and  $R_T$ , respectively), are responsible for the increased sensitivity and slower time courses of response (DeVoe, 1967; also the analysis of slow desensitization of linear responses by Fuortes and Hodgkin, 1964). In other words, at each steady state of light adaptation there will be different values of  $\tau_e$ ,  $\tau_T$ , and  $V_o$ . All other parameters will remain constant. At present it is not possible to say what the dynamics of change of  $\tau_e$  would be upon going from one level of background illumination to another. Were these dynamics known, then the output of the final exponential delay stage would be known too and the variations of  $\tau_T$  and  $V_o$  in the model could be calculated from the above equations.

To normalize the variables in the above equations, define  $(\tau_T)_o$  and  $P_o$  from equations (5) and (9), respectively, by setting  $I = I_o$  and  $V = V_o$  for any  $I_o$ . (As above, the subscript  $o$  denotes the value of a variable at an initial back-

ground illumination but not the value of the variable at any particular background illumination.) The normalized variables in the analogue are then

$$\bar{V} = V/V_o \quad (11)$$

$$\bar{I} = I/I_o \quad (12)$$

$$\bar{P} = P/P_o = \bar{V} \cdot \bar{I} \quad (13)$$

$$\bar{\tau}_T = \tau_T/(\tau_T)_o = \bar{V}/\bar{I} \quad (14)$$

By definition, the initial condition for each normalized variable is 1.

Equations (4), (6), and (7) can now be rewritten in terms of the above normalized variables:

$$\bar{\tau}_T = c_1 \exp [\bar{c}_2/(\bar{P}/\bar{c}_3 + 1)] \quad (15)$$

where the  $c$ 's are now determined from plots of normalized short-term DC response  $\bar{V}$  vs. normalized changes in background illumination  $\bar{I}$ . One such plot was given in the previous paper (DeVoe, 1967), and the solid line in that plot was fitted using equation (15). By analogy with equation (10) above,

$$\frac{d\bar{\tau}_T}{dt} = -\bar{\tau}_T \left( \frac{\bar{c}_2}{\bar{c}_3} \right) \left( \frac{1}{\bar{P}/\bar{c}_3 + 1} \right)^2 \frac{d\bar{P}}{dt} \quad (16)$$

Similarly, and keeping in mind that  $V_o = I_o A \tau_e^n (\tau_T)_o$ , equation (4) becomes

$$\frac{d(V/V_o)}{dt} + \frac{(V/V_o)}{\tau_T} = \frac{I_o [1 + mS(t)] A \tau_e^n}{I_o A \tau_e^n (\tau_T)_o}$$

where  $m = \frac{\Delta I}{I_o}$

or

$$(\tau_T)_o \frac{d\bar{V}}{dt} + \frac{\bar{V}}{\bar{\tau}_T} = 1 + mS(t) \quad (17)$$

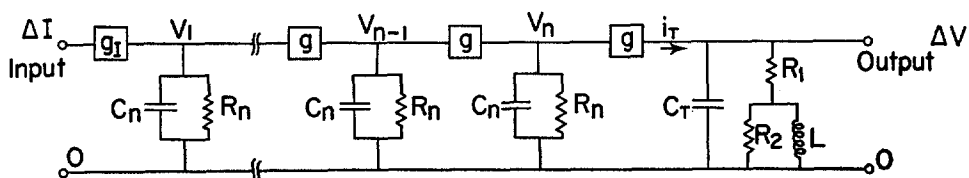
Finally, upon dividing both sides of equation (7) by  $P_o$ , and since from equation (8)  $P_o = V_o^2/(\tau_T)_o$ , there results

$$T \frac{d\bar{P}}{dt} + \bar{P} = \frac{\bar{V}^2}{\bar{\tau}_T} \quad (18)$$

The form of the equations is thus essentially unaltered.

*Incremental Responses of the Analogue* The above equations contain a number of parameters and time constants which, in this relatively complex

analogue, can only be determined from the fit of the incremental version of the analogue to linear responses of the spider eye. The linear, incremental behavior of  $R_T$  when it is biased with a steady current  $(i_T)_o$  (due to  $I_o$ ) is that of a resistance in series with a parallel resistance and inductance, as in the linear analogue in Fig. 3. (The proof of this equivalence is involved; see Ekelöf and Kihlberg, 1954; Mauro, 1961.) The instantaneous impedance of the  $RL$



$$T(s) = k \frac{\left(\frac{s}{Z} + 1\right)}{\left(\frac{s}{\omega_T}\right)^2 + 2\zeta\frac{s}{\omega_T} + 1}\left(\frac{s}{\omega_n} + 1\right)^n$$

$$\frac{1}{\omega_n} = \tau_e = R_n C_n$$

$$\frac{1}{Z} = \frac{L}{\left(\frac{R_1 R_2}{R_1 + R_2}\right)}$$

$$\frac{1}{\omega_T} = \sqrt{L C_T \frac{R_1 + R_2}{R_2}}$$

$$\frac{2\zeta}{\omega_T} = \frac{L}{R_2} + R_1 C_T$$

FIGURE 3. An analogue for linear incremental responses from light-adapted wolf spider eyes. The transfer function in the Laplace transform variable  $s$  is given in the top equation; the relations of its various parameters to the elements in the analogue are given in the bottom four equations. See text for further details.

network in Fig. 3 is  $(R_1 + R_2)$ . This is the same as the instantaneous impedance of  $R_T$  in Fig. 2 at  $I_o$ . Therefore,

$$(R_1 + R_2)C_T = (\tau_T)_o \quad (19)$$

In the middle of Fig. 3, the transfer function for the linear analogue is given in terms of the Laplace transform variable  $s$  (see Appendix III). This transfer function can be fitted to frequency response data of the spider eye (see Results,

below) and so all the parameters in the transfer function can be determined. In turn, by means of the equations at the bottom of Fig. 3, these parameters are related to the  $R$ 's,  $L$ , and  $C$ 's of the analogue. Upon solving and substituting in equation (19),

$$(\tau_T)_o = \frac{1}{2\zeta\omega_T - z} \quad (20)$$

The steady-state incremental value of  $R_T$  becomes, in the linear analogue in Fig. 3,  $R_1$ . Therefore, from equation (5),

$$\Delta V = \Delta I \cdot A \tau_e^n \cdot R_1 C_T \quad (21)$$

Solving the equations at the bottom of Fig. 3 for  $R_1 C_T$ :

$$R_1 C_T = \frac{z}{\omega_T^2} \quad (22)$$

It follows from equations (21) and (22) that  $A$  can be determined from the linear dc step response  $\Delta V$  and the parameters found by fitting the transfer function in Fig. 3 to frequency response data.

Once  $A$  is determined, the background potential  $V_o$  can be calculated solely from linear responses of the eye. Upon combining equations (5) and (20), there results

$$V_o = \frac{I_o \cdot A \tau_e^n}{2\zeta\omega_T - z} \quad (23)$$

Finally, the "thermal" time constant  $T$  can be related to the "electrical" time constant  $T_e$  of the linear analogue. The electrical time constant is  $L/R_2$  in the analogue in Fig. 3 and is found, upon solving the equations there, to be

$$T_e = \frac{2\zeta}{\omega_T} - \frac{z}{(\omega_T)^2} \quad (24)$$

This electrical time constant is related to the thermal time constant by means of the dynamic factor,  $F$  (Ekelöf and Kihlberg, 1954) which is defined as

$$F = \frac{R - r}{R + r} \quad \begin{array}{l} R = \text{static resistance} \\ r = \text{slope resistance} \end{array} \quad (25)$$

For the eye analogue at the ambient background illumination  $I_o$ ,  $R = R_T \propto V_o / I_o$  and  $r = R_1 \propto (\Delta V / \Delta I)_o$ . The proportionality constant is the same for both of the above equations (see equations (5) and (21)). Then, the thermal time constant is related to the electrical time constant and the dynamic factor as

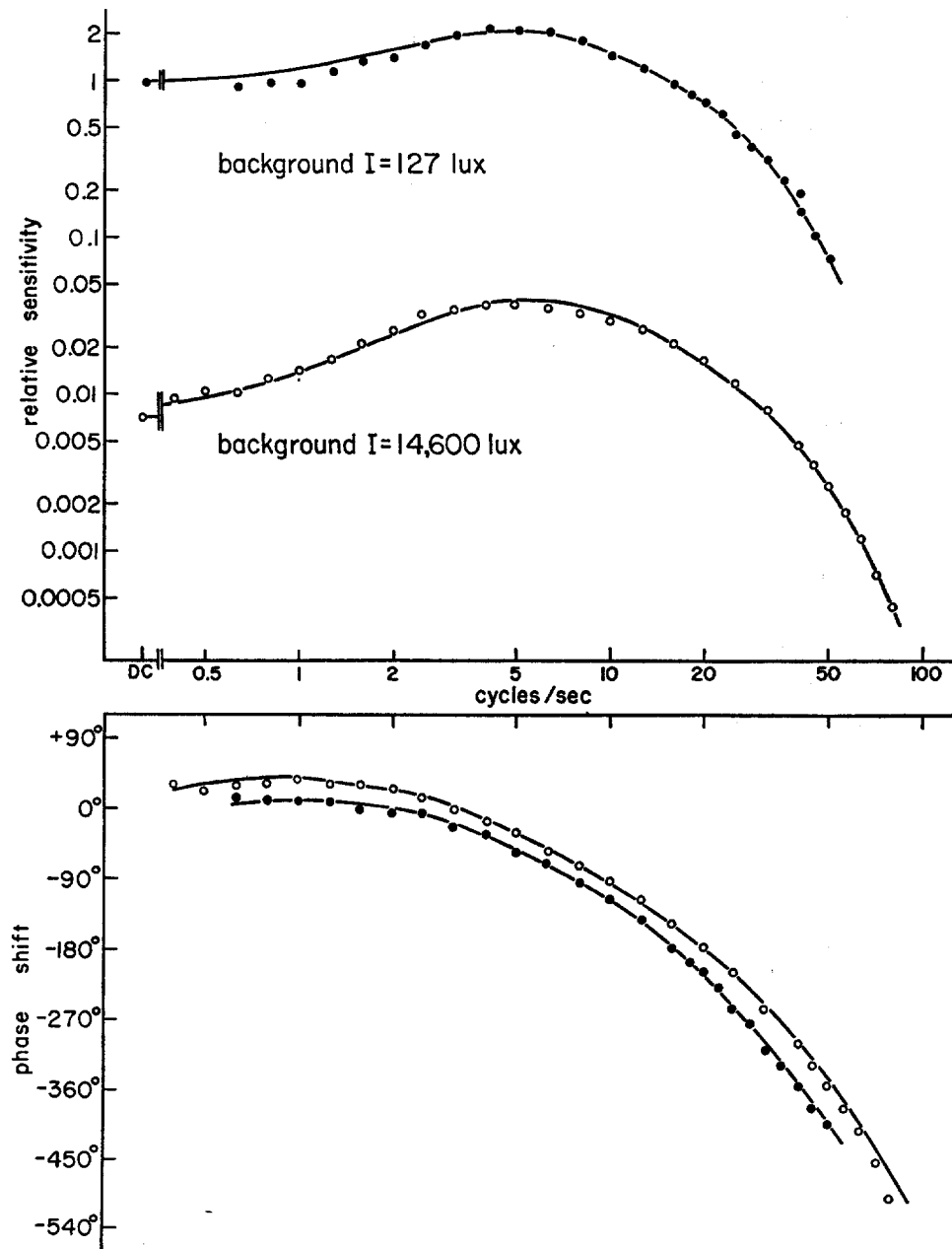


FIGURE 4. Frequency responses of two eyes of one wolf spider recorded in two different experiments at two background illuminations. For the background illumination of 14,600 lux, the left posterior median eye was used; for the background illumination of 127 lux, the right posterior median eye was used. Abscissas, frequency of sinusoidal modulation of the background illumination is plotted in cycles per second on a logarithmic scale. Upper ordinate, sensitivities of response at different frequencies and back-



follows:—

$$T = (1 + F)T_0 \quad (26)$$

(Ekelöf and Kihlberg, 1954. The proof of this follows from the proof that the *RL* network in Fig. 3 describes the incremental behavior of the time-variant resistance  $R_T$ ). Therefore, upon combining equations (24) to (26),

$$T = \left[ \frac{2\xi}{\omega_T} - \frac{z}{(\omega)_T^2} \right] \left[ \frac{2V_0/I_0}{V_0/I_0 + (\Delta V/\Delta I)_0} \right] \quad (27)$$

The value of  $T$  can thus be determined from experimentally found parameters.

#### EXPERIMENTAL RESULTS

*Linear Responses to Sinusoidal and Step Stimuli* Typical frequency sensitivities and phases of responses to sinusoidal modulation of background illumination are shown in Fig. 4 as open and filled circles. These data show the same dependence on amount of background illumination as do “deLange curves” from the human eye (deLange, 1961; Kelly, 1964) and as do frequency response curves from the eyes of flies (Kuiper and Leutscher-Hazelhoff, 1965) and *Limulus* (Pinter, 1966). At the higher background illumination, the eye is, of course, less sensitive, but it also has a higher frequency response and a greater amount of peaking.

The solid lines were fitted to the points using the transfer function given in Fig. 3. It can be seen that the fit is very good. Equally good fits have been obtained in 10 other experiments, although, of course, there has been considerable variation in the parameters from experiment to experiment. The

---

ground illuminations relative to the short term dc sensitivity at 127 lux background illumination are given on a logarithmic scale. The sensitivities were determined as the reciprocals of the per cent modulations of the background illuminations required to elicit 10  $\mu$ v peak-to-peak responses, where per cent modulation is defined as half the peak-to-peak stimulus amplitude divided by the mean or background illumination. Lower ordinate, on a linear scale are plotted phases of sinusoidal responses relative to phases of sinusoidal stimuli, as determined by the method illustrated in Fig. 1. In both parts of the figure, the open and filled circles are experimental points, while the solid lines are fitted from the transfer function in Fig. 3 with the following parameters:

Background illumination	$z$	$\omega_T$	$\xi$	$\omega_n$	$n$
lux	$sec^{-1}$	$sec^{-1}$		$sec^{-1}$	
14,600	3.55	35.5	0.9	631	10
127	7.94	31.6	1.0	501	10

multiple poles in the transfer function, due to the cascaded exponential delay stages in the linear analogue, dominate at high frequencies and predict well the recorded responses there. Likewise, the low frequency peaking is well described by the *RLC* network in the analogue. The peaking is usually sufficiently sharp that a damping factor less than 1 in the transfer function is needed. Finally, there is phase lead at low frequencies (Tables I and II). The frequency response of the RC feedback model (Pinter, 1966) would show peaking but not this phase lead, whereas the analogue does describe the phase lead. As mentioned earlier, this is one reason that the RC feedback model is felt to be inapplicable to the responses of light-adapted spider eyes.

The changes in the parameters of the analogue required to fit the data at the two background illuminations are in the directions expected. For one thing, the inductive behavior of the time-variant resistance in the analogue decreases as the current ( $i_T$ ), due to  $I_o$ , decreases (Mauro, 1961). This is consistent with the decreased peaking observed at the lower background illumination. Second, at the lower steady-state background illuminations,  $\tau_o$  and  $R_1C_T$  have increased, as found from lowered frequency responses. These increased time constants would, from equation (21), be expected to result in increased sensitivity of the eye (cf. the linear analysis of Fuortes and Hodgkin, 1964). In some but not all experiments, the increases in sensitivity at lower background illuminations could be completely accounted for, within experimental error, by these time-constant changes.

The linear analogue in Fig. 3 can also be tested by its ability to correctly predict the recorded responses to small incremental step stimuli. In Fig. 5 are shown linear step responses recorded in the same experiments as the responses in Fig. 4. The open circles make up the averaged recorded responses, and the solid lines are the step responses computed from the transfer functions used to obtain the solid lines in Fig. 4. Again, the agreement is excellent between the data and the linear analogue.

One final test may be made of the analogue using data based on linear responses. From equation (23),  $V_o$  can be calculated, and this calculated value can be compared with that measured as the dc response to turning off the background illumination. In one experiment,  $V_o$  measured was 293  $\mu v$  vs. 284  $\mu v$  calculated, while for another experiment,  $V_o$  measured was 537  $\mu v$  vs. 504  $\mu v$  calculated. These differences are well within the range of variations which may be expected from frequency response curve fitting. In addition, in experiments in which  $V_o$  has not been measured, the value of  $V_o$  calculated by equation (23) also appears consistent with measured responses. Thus, in Fig. 5 of the preceding paper (DeVoe, 1967), the crosses representing per cent dc responses were obtained using a  $V_o$  calculated from equation (23) to normalize the measured incremental short term dc responses to large step

stimuli. The resulting per cent DC response curve was in all respects comparable to those using measured values of  $V_o$ .

*Short-Term Nonlinear DC Responses* One example of short-term DC responses, such as were illustrated in the previous paper (DeVoe, 1967), is shown in Fig. 6. The open circles represent the short-term DC response  $V_o + \Delta V$  elicited by step stimuli  $\Delta I$ ; the total background illumination  $I_o + \Delta I$  is given in relative measure on the abscissa. These short-term DC responses show the nonlinearities ascribed to  $R_T$  in the analogue. They can be described with the equations which define the behavior of  $R_T$ ; combining equations

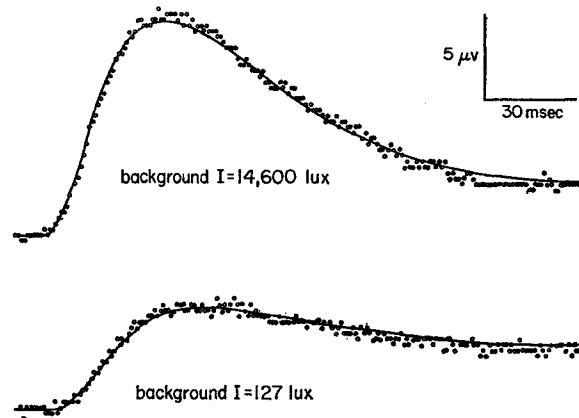


FIGURE 5. Linear step responses of light-adapted wolf spider eyes recorded in the same experiments as in Fig. 4. Upper figure, the open circles make up the average of 128 recorded responses to +8% steps; the solid line represents the response calculated from the transfer function fitted to the open circles in Fig. 4. Lower figure, the open circles make up the average of 128 recorded responses to +10% steps; the solid line represents the response calculated from the transfer function fitted to the filled circles in Fig. 4. Sampling time per point was 0.944 msec in both parts of the figure. In this and the following figures showing transient responses, negativity of the cornea of the illuminated eye with respect to the indifferent electrode is upward.

(5) and (6),

$$V_o + \Delta V = [I_o + \Delta I] A r_e^n \cdot \left[ c_1 \exp \left( \frac{c_2}{P/c_3 + 1} \right) \right] \quad (28)$$

For the curve-fitting procedure,  $P$  is obtained from equation (9), and the  $c$ 's are then found using a nonlinear parameter, least squares estimation routine (Marquardt, 1963). The solid line represents the resulting fit of equation (28) to the experimental data. (The solid line in Fig. 2 of the preceding paper (DeVoe, 1967) was also obtained using equation (28).) The fit of the line to the points is satisfactory, although some differences exist between them.

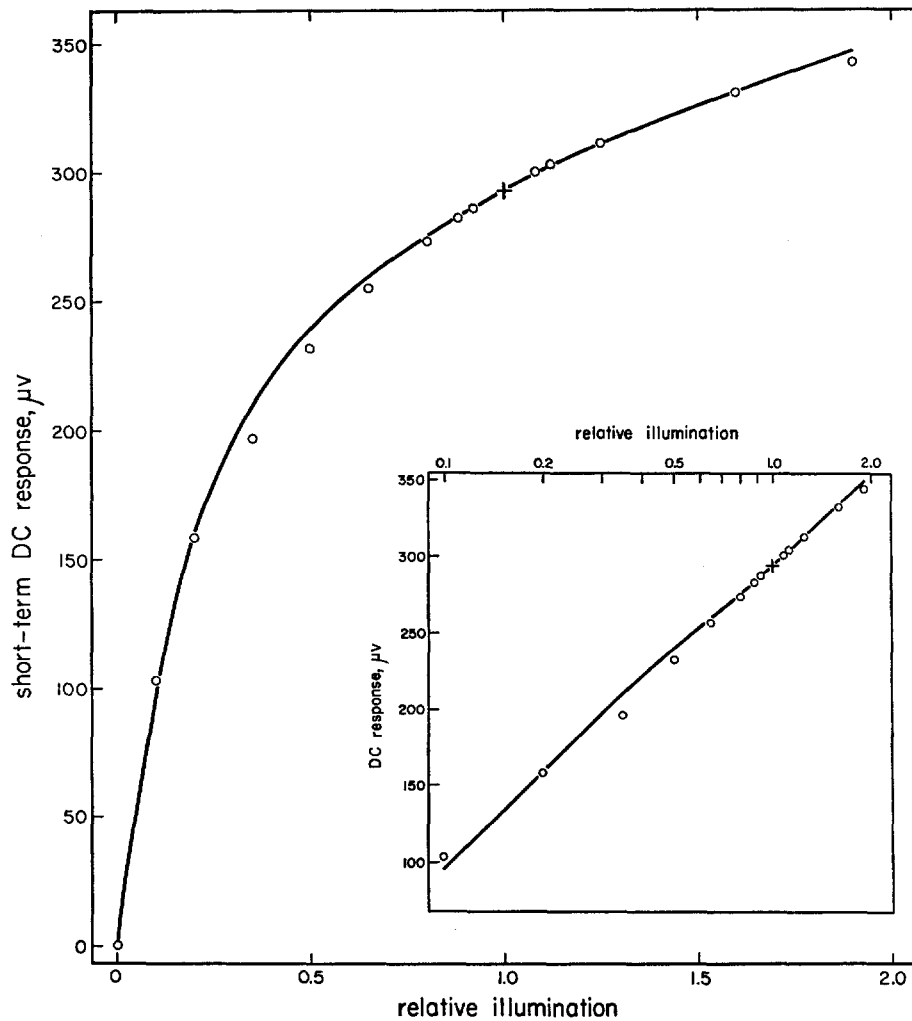


FIGURE 6. Short-term DC responses to step changes in background illumination. The cross represents the original base line in the light from which all short-term DC responses  $\Delta V$  (open circles) were measured. The bottom point is the DC response to turning off the background illumination. The difference between this bottom point and the cross is taken to be  $V_o$ , the background potential ( $293 \mu v$  in this experiment). All other DC responses are plotted with reference to the bottom point, the base line in the dark, as  $V_o + \Delta V$ . The illumination on the abscissa is given relative to the background illumination  $I_o$  of 12,100 lux as the sum of  $I_o$  and  $\Delta I$ , the step change in background illumination. The solid line was fitted to the data using equation (6) with the following constants:  $c_1 = 9.90$ ,  $c_2 = 2.42$ ,  $c_3 = 2526$ . Inset, the same data points and solid line have been replotted *vs.* relative total illumination on a logarithmic scale. The short-term DC responses are nearly a linear function of the logarithm of the total illumination except for lower total illuminations than used here.

These differences are probably due to the curve-fitting procedure ( $V$  appears as a dependent variable in equation (28) but as an independent variable in equation (9) used to calculate  $P$ ). As shown in the inset, both recorded and theoretical DC responses are nearly linear functions of the logarithm of total illumination. However, as explained in the previous paper (DeVoe, 1967), a logarithmic function breaks down as steps approach  $-100\%$ . The theoretical function (equation 28) on the other hand depends on the short-term DC response to the  $-100\%$  step, since this gives  $V_o$  (DeVoe, 1967). Thus the theoretical function, to which the dynamics of response may be related as well, is to be preferred.

*Calculation of Nonlinear Transient Responses* The above has illustrated that it is possible to fit the analogue to linear responses and to short-term nonlinear DC step responses of the light-adapted spider eye. From the parameters used in this curve fitting, it is now possible to make a prediction about what the nonlinear transients in step responses should be, as these have not been used in the curve-fitting procedure. To recapitulate, the equations to be used for these calculations are:

$$\frac{dV}{dt} + \frac{V}{\tau_T} = [I_o + \Delta I \cdot S(t)] A \tau_e^n \quad (4)$$

$$T \frac{dP}{dt} + P = \frac{V^2}{\tau_T} \quad (7)$$

$$\frac{d(\tau_T)}{dt} = -\tau_T \left( \frac{c_2}{c_3} \right) \left( \frac{1}{P/c_3 + 1} \right)^2 \frac{dP}{dt} \quad (10)$$

The values of  $A \tau_e^n$  and  $T$  are found from such linear frequency response data as were shown above using equations (21) and (26), respectively, while the  $c$ 's are found as in the previous section. The initial conditions are

$$V = V_o$$

$$\tau_T = \frac{V_o}{I_o A \tau_e^n} \quad (5)$$

$$P = I_o V_o A \tau_e^n \quad (9)$$

The equations were solved on the 7094 computer using a Runge-Kutta method. As a check on them, they were first used to predict the linear responses to small incremental step stimuli; one such prediction is shown in Fig. 7. It may be seen that the initial portion of the recorded responses (represented by the open circles) is well predicted, but that the predicted response is a bit too oscillatory in its decline from the peak response. Next, the equations were

used to predict responses to large step changes in background illumination; these are shown in Fig. 8 as the open circles superimposed upon the averaged recorded responses, denoted by the solid lines. The agreement between recorded and calculated responses seems quite good. As with the predicted linear response in Fig. 7, the agreement is worst in the decay from the peak. The calculated responses decay too rapidly after the peak. On the other hand, attempts to fit the peak decays better lead to too large predicted peak amplitudes.

The predicted response to the  $-100\%$  step also decays too rapidly and diverges from the recorded responses at the inflection point of the latter, a sort of peak. In other experiments, however, the agreement between predicted

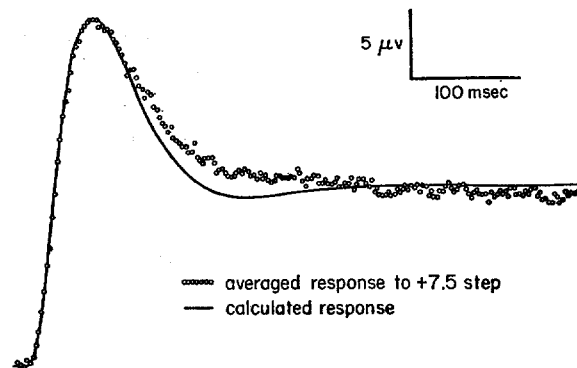


FIGURE 7. Averaged recorded linear step response and linear response predicted from the nonlinear analogue. The open circles make up the average of 128 recorded responses to a  $+7.5\%$  step change in a background illumination of 14,600 lux. The solid line was calculated using equations (4), (7), and (10); for details, see caption for Fig. 8. The response is drawn with respect to the base line in the light for clarity. Sampling time per point was 2.624 msec.

and recorded responses to  $-100\%$  steps was often much better, particularly at background illuminations lower than those used for the experiment in Fig. 8. Except for these complications, delayed nonlinearities due to a time-variant resistance in the nonlinear analogue duplicate well the nonlinear transients in step responses of the light-adapted spider eye.

*Sensitivity, Speed of Response, and Degree of Adaptation* Reduced light adaptation makes the eye more sensitive but slower in response. As pointed out above, these slower responses are described at steady state by increased time constants in the linear responses, and for some (but not all) cases, the increases in sensitivity were accounted for by the increased time constants. The same may be tested for nonlinear responses. The responses in Fig. 8 were recorded at an initial background illumination of 14,600 lux; in the same

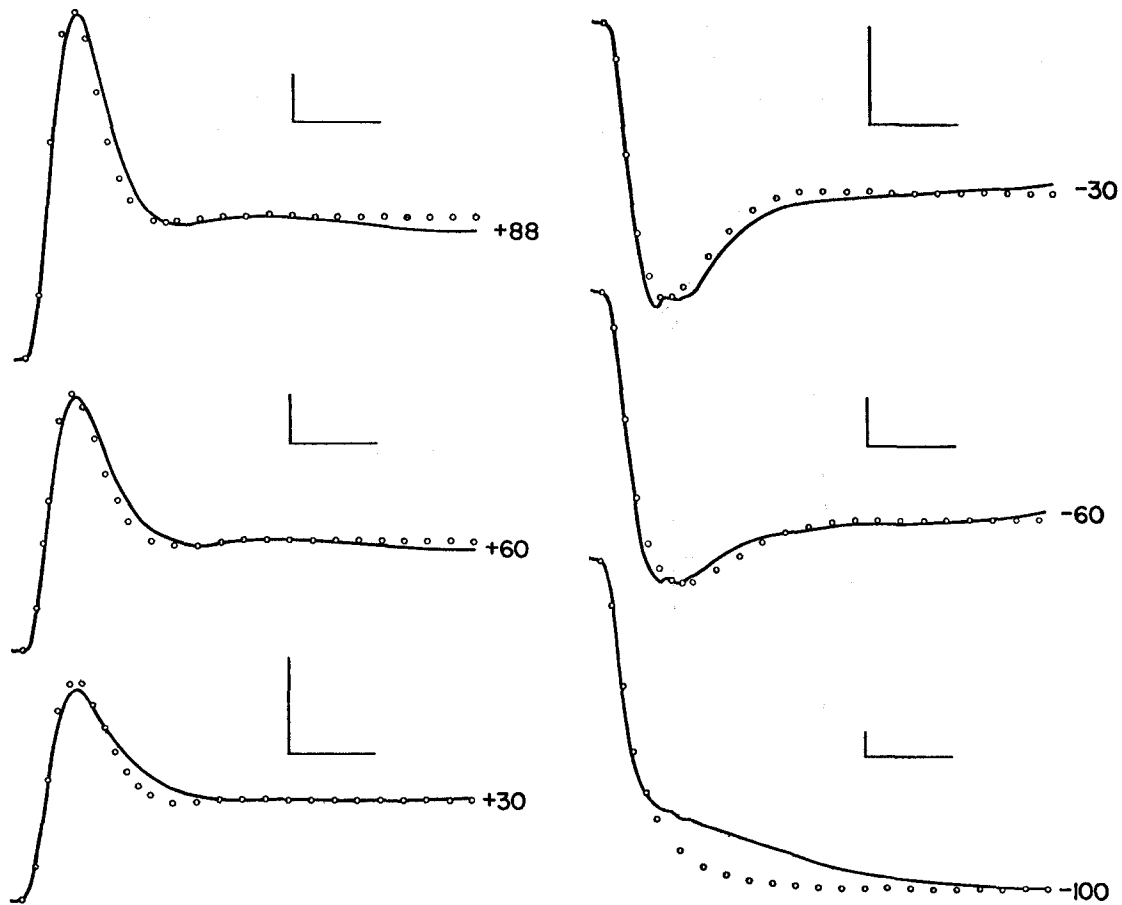


FIGURE 8. Averaged recorded and calculated nonlinear short-term step responses of a strongly light-adapted wolf spider eye. The solid lines represent the averages of from 16 to 32 responses to step changes in a background illumination of 14,600 lux; the sizes of these step changes as per cents of the background illumination are given to the right of each response. The open circles represent responses of the nonlinear analogue calculated from equations (4), (7), and (10). In these calculations,  $V_o = 537 \mu\text{v}$ ,  $A\tau_e^n = 18.0$ ,  $\tau_e = 3.162 \text{ msec}$ ,  $n = 7$ ,  $T = 53.8 \text{ msec}$ ,  $c_2 = 2.36$ , and  $c_3 = 22,429$ . For clarity, the responses have been drawn with respect to the base line in the light. The vertical calibrations represent  $40 \mu\text{v}$ ; the horizontal calibrations represent 100 msec.

experiment, step responses only were recorded at a background illumination of 400 lux. On the assumption that between the two states of adaptation, only the steady-state values of  $R_T$  and  $R_n$  (and not,  $n$ ,  $T$ , or  $A$ ) in the analogue had changed, then these changes were related by equation (5):

$$(\tau_e)_o^n (\tau_T)_o = \frac{I_o}{V_o A} \quad (29)$$

In equation (29),  $V_o$  is the background potential at the background illumination  $I_o$  of 400 lux, but  $n$  and  $A$  have values determined from frequency analysis at the background illumination of 14,600 lux. From just the nonlinear transient responses recorded at 400 lux background, there is no good way of

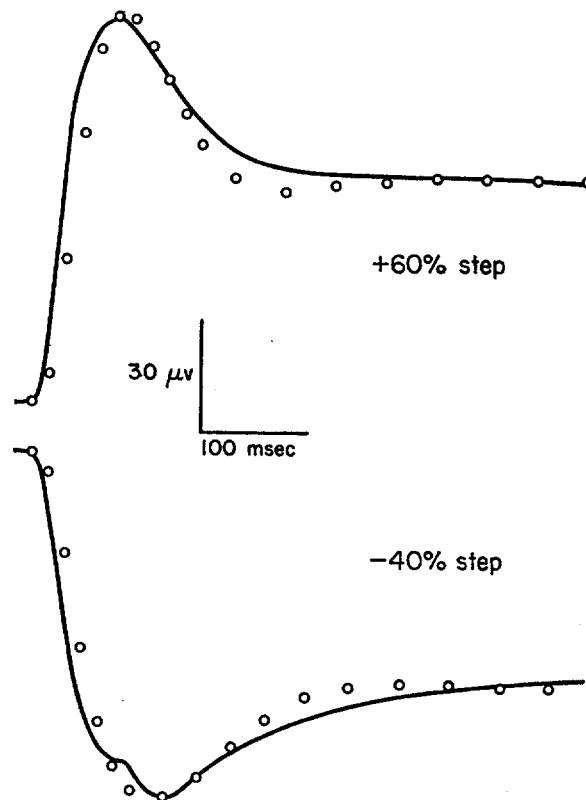


FIGURE 9. Averaged and calculated nonlinear short-term step responses from a moderately light-adapted wolf spider eye. The solid lines represent 32 averages of step responses recorded at a background illumination of 400 lux in the same experiment as in Fig. 8. The open circles are proportional to responses calculated from equations (16), (17), and (18), using the following values:  $\tau_e = 4.60$  msec,  $n = 7$ ,  $T = 53.8$  msec,  $(\tau_T)_o = 52.5$  msec,  $\bar{c}_2 = 1.99$ , and  $\bar{c}_3 = 1.20$ . (For comparison,  $(\tau_T)_o$  for the background illumination of 14,600 lux in Fig. 8 equaled 30.0 msec.) To obtain the calculated responses illustrated by the open circles, the calculated values of  $\bar{V}$  were multiplied by the measured value of  $364 \mu\text{v}$  for  $V_o$ .

determining the best values of  $(\tau_T)_o$  and  $(\tau_e)_o$ . Therefore pairs of values of these two time constants were found from equation (29) and used for solving equations (16) to (18). The best fit to the recorded responses obtained by this trial and error time constant determination is illustrated in Fig. 9. The calculated responses (open circles) are a reasonable approximation to those re-



corded (solid lines), although the decay from the peaks is again too rapid in the calculated responses. In addition, the latent periods of the calculated responses are a bit too long. These discrepancies are no more serious than in Fig. 8, however. Fig. 9 thus provides some evidence that between different steady states of light adaptation, only the shunt resistances  $R_n$  and  $R_T$  (i.e., the time constants  $\tau_e$  and  $\tau_T$ , respectively) in the analogue have changed (by one means or another). That is, the measured steady-state sensitivities  $V_o/I_o$  can be divided up among the time constants according to equation (29). This bears out similar conclusions reached from linear analysis of small amplitude flash responses of light- and dark-adapted *Limulus* ommatidia (Fuortes and Hodgkin, 1964). These workers, however, used a simpler analogue consisting solely of exponential delay stages with all but one section having a time constant varied by light adaptation.

*Nonlinear Responses Not Predicted by the Analogue* There are several aspects of nonlinear responses from light-adapted wolf spider eyes which cannot be accounted for by the nonlinear analogue. First, in the peaks of responses to negative step changes in background illumination, there are notches which do not appear in the predicted responses (Figs. 8 and 9). The predicted response to a  $-100\%$  step diverges from the recorded response at just about the point where the notches appear in responses to smaller negative steps. Likewise, in comparing scaled-up linear responses (to small negative steps) with nonlinear responses actually elicited by large negative steps, it was found that the recorded responses become nonlinear at about the time the notches were generated (DeVoe, 1967). All this could mean that there were two processes, one delayed with respect to the other, which added together to yield the observed nonlinear responses. Such a conclusion would be at variance with the nonlinear analogue developed above, which supposes that there is only one, smoothly changing, nonlinear process.

A second aspect of nonlinear responses which cannot be accounted for by the nonlinear analogue occurs upon terminating a negative step and may be seen in Fig. 10. The solid line is the averaged response to a  $-100\%$ , 315 msec flash, and the open circles represent the response predicted from the nonlinear analogue. The recorded response to the end of the period of darkness returns to the original base line much more rapidly than does the predicted response, its rate of rise becomes faster, its frequency of oscillation is greater, and the damping appears to be much less. A similar disparity between recorded and calculated responses to the end of a 250 msec,  $-80\%$  flash has also been seen. In the latter, however, the disparity was smaller and the recorded response took longer to settle down than did the end of the response in Fig. 9. On the other hand, after the largest possible positive flash ( $+90\%$ ), the recorded end response had a large undershoot of the original base line which

decayed away at the same rate as did the predicted response (although there was a bit more undershoot in the predicted response).

Finally, there is the point made repeatedly above, namely, that the rate of decay from the peaks of responses, particularly in the peaks of responses to positive step stimuli, is too great in the predicted responses. Although this is not serious in most of the predicted responses illustrated in Figs. 7 to 9, it becomes quite serious when attempting to predict responses recorded at the lowest background illuminations used (about 12 lux). Responses to positive steps, even small positive steps, have too great a rate of rise and too slow a de-

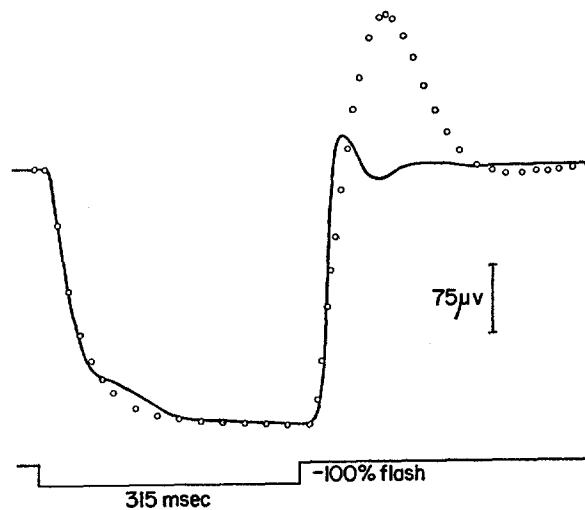


FIGURE 10. Failure of the nonlinear analogue to predict the end response to a negative flash. The solid line represents the average of 32 recorded responses to turning off the background illumination of 12,100 lux for 315 msec ( $-100\%$  flash). Downward in the line at the bottom of the figure indicates when the light went off, upward when it went back on. The open circles represent the response of the nonlinear analogue to this  $-100\%$  flash calculated using equations (4), (7), and (10). For the calculations,  $V_o = 293 \mu\text{v}$ ,  $A\tau_e^n = 9.10$ ,  $\tau_e = 1.41 \text{ msec}$ ,  $n = 10$ ,  $T = 95.6 \text{ msec}$ ,  $c_2 = 2.42$ , and  $c_3 = 2526$ .

cay from the peak to be predicted by the nonlinear analogue. On the other hand, responses to negative steps recorded at these low background illuminations can be predicted from the analogue. Perhaps a different analogue for delayed nonlinearities than one based on the dynamics of a time-variant resistance might have led to more consistent predictions. Alternatively, perhaps at these low background illuminations there are processes in addition to such dynamics which contribute to the nonlinearities in response.

#### DISCUSSION

*Physiological Implications of the Nonlinear Analogue* The above results provide quantitative support for the schema introduced in the previous paper to

explain undershoots and nonlinearities in step responses of light-adapted wolf spider eyes. The thrust of that schema was that the nonlinearities took time to develop and hence led to the overshoots in step responses. In the present paper, it has been argued that the dynamics of such short-term (one-half sec or less) nonlinearities can be duplicated by a single stage in an eye analogue. This is to be compared with the involvement of all 10 (or so) stages in the nonlinear RC feedback model for the *Limulus* eye (Fuortes and Hodgkin, 1964). One question now is whether this single nonlinear stage in the spider

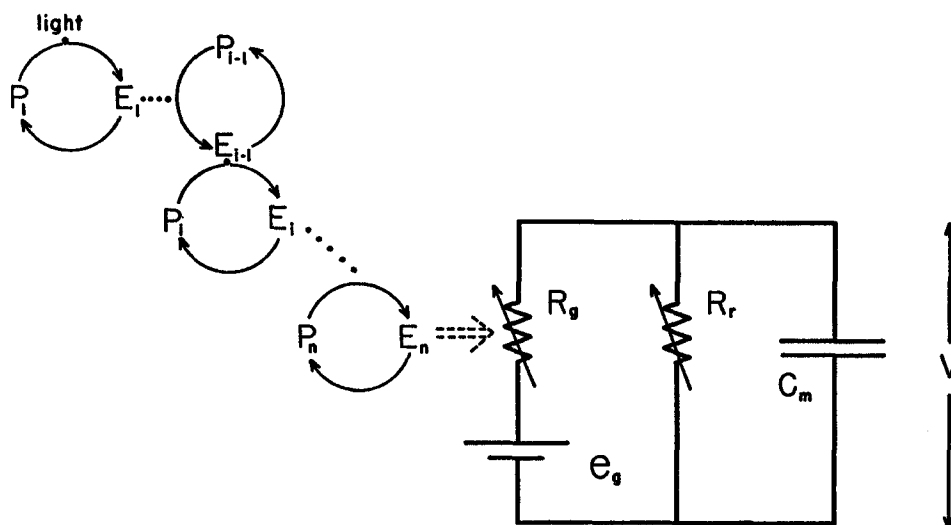


FIGURE 11. A model for the visual receptor cell. The effect of light is amplified by the cascaded chemical reactions  $P_i \rightarrow E_i$ , all of which are assumed to have the same kinetics. The conductance  $\frac{1}{R_g}$  changes in proportion to the concentration of the final chemical product  $E_n$ . In the equivalent circuit for the membrane,  $e_0$  is the excitatory equilibrium potential,  $R_r$  is the resting membrane resistance,  $C_m$  is the membrane capacity, and all potentials are measured with respect to the resting potential. See text for further details.

eye analogue could correspond to a single physiological process in the eye, such as activation of receptor cell membranes. Likewise, the stages of exponential delay in the analogue ought also to have some physiological explanation.

To see what it would mean if short-term nonlinearities were indeed due to receptor cell membrane dynamics, consider the properties of a possibly more physiological model diagrammed in Fig. 11. This model will serve to illustrate what could lie behind the properties of the analogue derived above. It is, of course, only one of many possible physiological models and, as will be mentioned below, is neither complete nor necessarily the best to explain all the available data. In the model, light is supposed to convert a spider rhodop-

sin (DeVoe and Zvargulis, 1967)  $P_1$  to an enzyme  $E_1$ , which in turn converts a second proenzyme  $P_2$  to a second enzyme  $E_2$ , and so on (Wald, 1965). The final enzyme  $E_n$  would then be supposed to change the resistance  $R_g$  of the receptor cell membrane. The electrical equivalent circuit of this cell membrane is adapted from that for *Limulus* eccentric cells (Fuortes, 1959; Rushton, 1959). However, the resting membrane potential has been ignored (Purple and Dodge, 1965); it would be represented otherwise by a battery  $E_r$  in parallel with the resting resistance  $R_r$ .

The dynamics of the physiological model in Fig. 11 can readily be related to those of the analogue in Fig. 2. To begin with, suppose that the rate of conversion of proenzyme to enzyme is proportional to the concentration of the preceding enzyme in the chain (or to the light  $I$  for  $P_1$ ), and that the rate of inactivation of enzyme is proportional to its own concentration. Then for the  $i$ th proenzyme-enzyme conversion,

$$\frac{dE_i}{dt} = (\alpha_i P_i) E_{i-1} - \beta_i E_i \quad (30)$$

where  $\alpha_i$  and  $\beta_i$  are rate constants. If  $P_i$  is present in such large concentrations that it is never limiting, then these dynamics are the same as those of the exponential delay stages in the analogue in Fig. 2. From equations (1) and (30), and supposing that  $v_i$  and  $E_i$  are the same variable,

$$\beta_i = \frac{1}{R_n C_n} \quad (31)$$

$$\alpha_i P_i = \frac{g}{C_n} \quad (32)$$

That the concentration of  $P_i$  might not be rate-limiting could follow from the observation that the concentration of rhodopsin, which would be  $P_1$  in the model, does not appreciably affect the light-adapted rat ERG threshold even when a very large per cent of it has been bleached away (Dowling, 1963). It is also not necessary to suppose therefore that enzyme is directly reconverted to proenzyme, only that it is inactivated at a rate proportional to its own concentration.

Continuing, the differential equation for the membrane equivalent circuit in Fig. 11 is

$$C_m \frac{dV}{dt} + \frac{V}{R_r} = \frac{e_0 - V}{R_g}$$

or

$$\frac{dV}{dt} + \frac{V}{C_m} \left( \frac{1}{R_g} + \frac{1}{R_r} \right) = \left( \frac{e_0}{C_m} \right) \frac{1}{R_g} \quad (33)$$

Comparing this with the equation for the last stage of the nonlinear analogue

$$\frac{dV}{dt} + \frac{V}{\tau_T} = \left(\frac{g}{C_T}\right) v_n \quad (3)$$

and supposing that  $C_T = C_m$ , then

$$\frac{1}{R_T} = \frac{1}{R_g} + \frac{1}{R_r} \quad (34)$$

$$g \cdot v_n = \frac{e_g}{R_g} \quad (35)$$

As above,  $v_n = E_n$ . It is therefore only necessary to make the conductance  $\frac{1}{R_g}$  proportional to the concentration  $E_n$  of the final product in Wald's (1965) enzyme amplification scheme in order that the analogue and the model have the same dynamics. This would not be unreasonable if the final product  $E_n$  were in fact an excitatory transmitter or its equivalent.

The dynamics of delayed nonlinearities in spider eye responses were embodied in  $R_T$  in the analogue. From equation (34), these dynamics are represented in the membrane equivalent circuit by the parallel behavior of  $R_g$  and  $R_r$ . This predicts that the membrane resistance of spider visual cells ( $R_g$  in parallel with  $R_r$ ) would be a function of the membrane potential, since  $R_T$  in the eye analogue is dependent upon the response voltage. If this prediction were true, then extrinsic current (passed through an intracellular electrode, for example) would be rectified by light-adapted spider visual cells according to a curve such as the one in Fig. 6. In the eccentric cell of *Limulus*, there is no such rectification of extrinsic current (Fuortes, 1959). However, rectification of extrinsic current has been observed in reticular cells of flies (Washizu, 1964), locusts (Scholes, 1965), and *Limulus* (Borsellino, Fuortes, and Smith, 1965). Moreover, in locust reticular cells, the full amount of such rectification is reached only after about 50 msec (Scholes, 1965). In other words, these reticular cells display delayed rectification.

A possible conclusion to be drawn from all this is that delayed rectification might occur in spider visual cells and might be responsible for the short-term, delayed nonlinearities illustrated above and in the previous paper (DeVoe, 1967). The dynamics of delayed rectification have been studied best in squid giant axons, in which they are due to the potassium conductance changes (Hodgkin and Huxley, 1952). Subthreshold stimulation of these axons by small current steps causes them to respond reactively as though they contained inductance (Cole, 1941). This inductance is also largely attributable to potassium conductance changes, which, when caused by incremental, subthreshold stimuli, can be represented by the same inductance-resistance net-

work as in the eye analogue in Fig. 3. Finally, the inductance due to potassium conductance changes diminishes as the membrane is hyperpolarized and disappears at the potassium equilibrium potential (Hodgkin and Huxley, 1952). As pointed out by Mauro (1961), a thermonegative time-variant resistance behaves analogously. When current-biased, it displays inductive reactance like that of potassium conductance changes, and at zero bias, the inductance disappears. In turn, this paper has shown how the spider eye responds analogously to a time-variant resistance (with that resistance placed in the analogue in Fig. 2). Although it is thus a long way around from extracellularly recorded spider visual responses to potassium conductance-like processes in spider visual cells, the point of developing the model in this paper has been to point up the comparison. Naturally it cannot be said from extracellular recordings what specific ion would be responsible for the hypothesized delayed rectification in spider visual cells. Likewise, it cannot be proven that such delayed rectification occurs at a membrane at all; it might reside, for example, in the kinetics of some excitatory transmitter release. Presumably these alternatives will be open to experimental test by intracellular recording techniques.

Unlike the above, the chemical part of the proposed model is not open to any obvious experimental test. The proenzyme-enzyme model of Waold (1965) is by no means the only one which would be consistent with the exponential delay behavior of the analogue in Fig. 2. Some alternative models must be considered. One such is the Ives (1922) diffusion model for temporal integration; this has, in effect, been reformulated by Rushton (1965) in terms of a leaky cable. In Rushton's model, the leakiness of the cable and hence the gain is a function of the output voltage. Such diffusion or cable models are necessarily very wasteful of whatever it is that is diffusing (Cobb 1934). Marimont (1965) and Borsellino, Fuortes, and Smith (1965) have developed models for flow of substances between compartments or along a chain of fixed sites; these models can be made to yield large steady-state changes in gain for small changes in time scale, such as occur in the eye. They do not, however, result in any absolute gain; that is, multiplication of the number of input events (quantum absorptions) at the outputs. Finally, Levinson (1966) has proposed a single-stage, stochastic model which might provide some absolute gain and which could easily be interpreted as representing the behavior of  $R_0$  in the model in Fig. 11. In addition, since it does not incorporate presumably fixed, cascaded reactions or stages, it is easiest to reconcile with the variability from preparation to preparation of the number  $n$  of such cascaded events needed to explain the dynamics of response. Thus, Fuortes and Hodgkin (1964) found that  $n$  could vary between 4 and 12 in *Limulus*. In the spider eye,  $n$  has generally been 10 (it was 7 in the experiments in Figs. 7-9), but in two experiments  $n$  changed from 10 to 7 when the background illumination was

decreased. It is felt that these changes were outside experimental error. Therefore, it remains uncertain whether  $n$  represents some number of chemical reactions, as the model in Fig. 11 would imply, and if so, how this number could vary.

*The Role of Exponential Delay Stages in Nonlinear Responses* The model developed in this paper describes only short-term (i.e., one-half sec long) transient responses. The model does not attempt to account for the later phenomenon of creep described in the previous paper (DeVoe, 1967). Creep has the following properties. First, it exists because the short-term DC responses are different from steady-state DC responses. Second, these differences become smaller as the eye is made less light-adapted. In dark adaptation, there are no differences and hence no creep; the DC response to a light is established in 1 to 2 sec. Third, it takes an estimated 12–15 sec for the response of a strongly light-adapted eye to creep from the short-term to the steady-state DC response. How long creep takes in a weakly light-adapted eye is not known.

In addition to creep, a second feature of the spider eye's dynamic responses needs to be accounted for. It was shown above that  $\tau_e$  (that is,  $R_n C_n$ ) in the analogue in Fig. 2 eventually increased after the background illumination had been decreased. In terms of the model in Fig. 11,  $\beta_i$  decreased (equation 31). What is not known is when  $\tau_e$  (or  $\beta_i$ ) began to change after the background illumination had been changed.

One economical way in which to explain creep would be to postulate now that it is due to changes in  $\tau_e$ , and that these changes occur most slowly in the strongly light-adapted eye but most rapidly in the dark-adapted eye. That is, slow changes in  $\tau_e$  result, from equation (2), in slow changes in sensitivity of the eye proportional to  $(\Delta\tau_e)^n$  (or  $\frac{1^n}{\Delta\beta}$ ). These sensitivity changes would then be reflected in changes in response voltage, that is, in creep. In the strongly light-adapted spider eye, in which creep begins 400–500 msec after a step change in background illumination, changes in  $\tau_e$  would have to be equally delayed. If they were thus delayed, it would explain why  $\tau_e$  could be taken to be constant above in analyzing frequency responses down to as low as 0.5 cps. Were  $\tau_e$  not so constant, then it might have contributed something to the peaking in frequency responses (Pinter, 1966). It was satisfactory to assume that it did not.

On the other hand, since the steady-state DC response of the dark-adapted spider eye to a light is reached in a second or so (DeVoe, 1967),  $\tau_e$  presumably would also reach its light-adapted value in this time. This presumption may provide a way to bring together, in part at least, the RC feedback model for the dark-adapted *Limulus* eye (Fuortes and Hodgkin, 1964; Marimont, 1965) and the present model for the light-adapted spider eye. As stated earlier,

the best form of the RC feedback model takes the feedback voltage from the next-to-last exponential delay stage (Marimont, 1965) and hence is potentially a two-part model, as is the present one. Similarly, a two-part model is implied by the finding of Fuortes and Hodgkin (1964) that in a linear analogue of small flash responses of the light-adapted *Limulus* eye, one (or two) stages of exponential delay were unaffected by "slow desensitization;" that is, these exponential delays kept the time constants they had in the dark-adapted eye. Conversely, perhaps the two-part spider eye analogue would have a dark-adapted behavior somewhat like that of Marimont's (1965) model, in that there would be feedback from the last exponential delay in Fig. 2 onto all other exponential delays (but not upon the last stage). It would be predicted that the inductive behavior of the time-variant resistance stage in Fig. 2 would disappear in the dark, when there would be no bias current  $i_T$  through  $R_T$  (Mauro, 1961). Then, this stage would appear as but another exponential delay section (although probably with a time constant larger than the other exponential delay stages). This has not yet been quantitatively tested. Likewise, RC feedback upon all but the last stage of the dark-adapted version of the spider eye analogue could perhaps explain why the steady-state DC response of the dark-adapted spider eye is achieved so fast. This possibility likewise awaits a quantitative test.

It can be seen from the above that some partial RC feedback in the dark-adapted spider eye need not be inconsistent with the model for the light-adapted spider eye developed in this paper. In terms of the chemical part of the model in Fig. 11, RC feedback would be equivalent to making all  $\beta$ 's proportional to  $\left(1 + \frac{E_n}{W}\right)$ , where  $W$  is a scaling constant (cf. Fuortes and Hodgkin, 1964). Why and how this proportionality would arise is an unanswered question. An altogether different question is why feedback of  $E_n$  on the  $\beta$ 's would be so slow in the light-adapted eye that it could be ignored in the present model, at least for the first half-sec of incremental response. In other words, if feedback of  $E_n$  on the  $\beta$ 's of the model in Fig. 11 causes them to change and hence causes creep in long-term responses of light-adapted eyes, this feedback must be very much slower than it is in the dark-adapted eye. Answers to questions like these will have to await further understanding of the exponential delay-like dynamics of spider eye retinal action potentials.

#### APPENDIX I

For a thermonegative, time-variant resistance (in particular, a thermistor), the DC resistance is a unique function of its absolute temperature  $\Theta$ :

$$R_T = R_\infty \exp [B/\Theta]$$

$B =$  a constant dependent on the thermistor material  
 $R_\infty =$  resistance when temperature is infinite



(Becker, Green, and Pearson, 1946). In turn, for such a resistance in which heat is dissipated solely by conduction and convection, the dissipated power  $P'$  is given by

$$P' = k(\Theta - \Theta_o) \quad \begin{array}{l} k = \text{dissipation constant} \\ \Theta_o = \text{ambient temperature} \end{array}$$

(Ekelöf and Kihlberg, 1954). Assuming that the ambient temperature remains constant, the temperature  $\Theta$  may be eliminated, yielding

$$R_T = R_\infty \exp \frac{B}{P'/k + \Theta_o} \quad (36)$$

Likewise, the power supplied to such a resistance (as for example by the current through it) is partly dissipated and partly used to heat it:

$$N = P' + H \frac{d\Theta}{dt} \quad \begin{array}{l} N = \text{supplied power} \\ H = \text{heat capacity} \end{array}$$

From the above,

$$\frac{dP'}{dt} = k \frac{d\Theta}{dt}$$

Therefore,

$$N = P' + T \frac{dP'}{dt}$$

$T = \frac{H}{k}$  = thermal time constant (Ekelöf and Kihlberg, 1954).

In terms of the analogue in Fig. 2, the supplied power is  $\frac{V^2}{R_T}$  so the above may be written

$$T \frac{dP'}{dt} + P' = \frac{V^2}{R_T} \quad (37)$$

There are too many parameters in the analogues in Figs. 2 and 3 for  $R_T$  to be determined from experimental data; however,  $R_T C_T = \tau_T$  may be specified, as was shown by equation (20) for example. Therefore (36) and (37) must be rewritten:

$$\tau_T = R_T C_T = c_1 \exp \left[ \frac{c_2}{P'/c_3 + 1} \right] \quad (6)$$

$$\begin{array}{l} P = P'/C_T \\ c_1 = R_\infty C_T \\ c_2 = B/\Theta_o \\ c_3 = k\Theta_o \end{array}$$

$$T \frac{dP}{dt} + P = \frac{V^2}{\tau_T} \quad (7)$$

## APPENDIX II

The "constants,"  $c_1$  and  $c_3$ , in the equation

$$\tau_T = c_1 \exp \left[ \frac{c_2}{P/c_3 + 1} \right] \quad (6)$$

change considerably with changes in background illumination, while  $c_2$  changes hardly at all. It has been shown (DeVoe, 1967) that one curve will fit normalized short-term DC responses at all background illuminations; the equation for this nor-

TABLE III  
THE RELATIONSHIPS BETWEEN THE PARAMETERS  $c$  IN EQUATION  
(6) AND THE PARAMETERS  $\bar{c}$  IN EQUATION (15)

See text for further details.

Background illumination	$c_1$	$(\tau_T)_o$	$c_1/(\tau_T)_o$	$c_2$	$c_3$	$P_o$	$c_3/P_o$
<i>lux</i>		<i>msec</i>					
14,600	7.52	35.8	0.210	2.09	5968	2020	2.95
14,600	5.78	30.0	0.193	2.36	22,429	9101	2.46
12,100	9.90	32.2	0.307	2.42	2526	2668	0.95
400	20.6	52.5	0.396	2.11	1950	2530	0.77
100	19.0	44.3	0.428	2.20	138	213	0.65
Values of $\bar{c}$ 's fitted to normalized short-term DC responses (DeVoe, 1967):							
			$\bar{c}_1$	$\bar{c}_2$			$\bar{c}_3$
			0.338	1.99			1.20

malized curve was equation (15) above. Upon comparing equations (6) and (15), it may be seen that

$$\bar{c}_1 = c_1/(\tau_T)_o$$

$$\bar{c}_2 = c_2$$

$$\bar{c}_3 = c_3/P_o$$

In Table III, data from five experiments at four different background illuminations have been used to calculate  $\bar{c}$ 's from the fitted  $c$ 's and observed  $P_o$ 's and  $(\tau_T)_o$ 's according to the above equations; these calculated  $\bar{c}$ 's may be compared with those fitted by least squares to normalized short-term DC responses (Fig. 5 in the preceding paper, DeVoe, 1967). There are considerable differences between the calculated and fitted  $\bar{c}$ 's, but these differences are smallest between the various values of  $c_2$ . The existence of one, normalized short-term DC response curve presumably depends, there-

fore, on the fact that all such curves have about the same shape, which is determined by  $c_2$ , but are adjusted to the ordinates and abscissas of plots such as Fig. 6 of this paper by the scale factors  $c_1$  and  $c_3$ . These scale factors then change to accommodate, within experimental error, values of  $P_o$  and  $(\tau_T)_o$  which change with background illumination.

### APPENDIX III

*The Differential Equations of the Linear Analogue* Fuortes and Hodgkin (1964) developed the linear equations for the exponential delay sections in the analogue of Fig. 3 and these will be merely stated here. Writing  $s = d/dt$  and  $\tau_e = R_n C_n$ , the relation between the input  $I$  and the output  $v_n$  of the final exponential delay section is given by

$$(\tau_e s + 1)^n \cdot v_n = \left(\frac{g}{C_n}\right)^n \cdot \tau_e^n \cdot I \quad (38)$$

The output  $V$  of the  $RL$  network is taken to be the measured response and is obtained as follows:—

$$C_T \frac{dV}{dt} + \frac{V - e_L}{R_1} = g \cdot v_n$$

As above,  $v_n$  is the output of the final exponential delay section, while  $e_L$  is the voltage across the inductance  $L$ . Solving for  $e_L$ ,

$$e_L = R_1 C_T \frac{dV}{dt} + V - R_1 \cdot g \cdot v_n \quad (39)$$

Likewise, the current across  $R_1$  is the sum of the currents through  $R_2$ , and  $L$ :

$$i_{R_1} = e_L/R_2 + 1/L \int e_L$$

and the output voltage  $V$  is given by

$$V = e_L + R_1 i_{R_1}$$

Upon eliminating  $i_{R_1}$  from the above two equations and differentiating,

$$L \frac{R_1 + R_2}{R_1 R_2} \frac{d}{dt} e_L + e_L = \frac{L}{R_1} \frac{dV}{dt} \quad (40)$$

Finally,  $e_L$  may be eliminated by substituting equation (39) and its derivative into equation (40); there results

$$LC_T \frac{R_1 + R_2}{R_1 R_2} \frac{d^2 V}{dt^2} + \frac{R_1 R_2 C_T + L}{R_2} \frac{dV}{dt} + V = g R_1 \left( L \frac{R_1 + R_2}{R_1 R_2} \frac{d}{dt} v_n + v_n \right) \quad (41)$$

Writing

$$z = \left( \frac{R_1 R_2}{R_1 + R_2} \right) / L, \quad \omega_T = 1 / \sqrt{LC_T \frac{R_1 + R_2}{R_2}}, \quad \frac{2\zeta}{\omega_T} = \frac{C_T R_1 R_2 + L}{R_2},$$

and  $\omega_n = 1/\tau_e$ , equations (38) and (41) may be combined to give

$$\left( \frac{s}{\omega_n} + 1 \right)^n \left( \left[ \frac{s}{\omega_T} \right]^2 + \frac{2\zeta s}{\omega_T} + 1 \right) \Delta V = \left( \frac{g}{C_n} \right)^n \left( \frac{g}{C_T} \right) \tau_e^n R_1 C_T \left( \frac{s}{z} + 1 \right) \Delta I \quad (42)$$

By taking the ratio of  $\Delta V$  to  $\Delta I$  and setting

$$k = \frac{g^{n+1}}{C_n^n C_T} R_1 C_T \tau_e^n \quad (43)$$

(assuming that all the  $g$ 's and  $c_n$ 's are equal), the transfer function given in the middle of Fig. 3 results.

The author wishes to thank Dr. K. E. Machin of Cambridge University for initially pointing out the resemblance of spider visual dynamics to those of time-variant resistance, Drs. R. Shephard and U. Gessner for helpful discussions while this work was in progress, the staff of the Everglades National Park, Florida for permission to collect some of the spiders used in this work, and Drs. J. Dowling, D. Robinson, and W. Marks for comments on the manuscript of this paper.

The computations with IBM equipment were done in the Computing Center of the Johns Hopkins Medical Institutions, which is supported by Research Grant FR-00004 from the National Institutes of Health.

This investigation was supported by United States Public Health Service Research Grant NB-03750 from the National Institute of Neurological Diseases and Blindness.

Received for publication 11 January 1967.

#### REFERENCES

- BECKER, J. A., C. B. GREEN, and G. L. PEARSON. 1946. Properties and uses of thermistors—thermally sensitive resistors. *Trans. Inst. Elec. Engrs.* **65**:711.
- BORSELLINO, A., M. G. H. FUORTES, and T. G. SMITH. 1965. Visual responses in *Limulus*. *Cold Spring Harbor Symp. Quant. Biol.* **30**:429.
- COBB, P. W. 1934. Some comments on the Ives theory of flicker. *J. Opt. Soc. Am.* **24**:91.
- COLE, K. S. 1941. Rectification and inductance in the squid giant axon. *J. Gen. Physiol.* **25**:29.
- DEVoe, R. D. 1963. Linear relations between stimulus amplitudes and amplitudes of retinal action potentials from the eye of the wolf spider. *J. Gen. Physiol.* **47**:13.
- DEVoe, R. D. 1964. Linear electrical flicker responses from the eye of the wolf spider. *Doc. Ophthalmol.* **18**:128.
- DEVoe, R. D. 1966. A non-linear model of sensory adaptation in the eye of the wolf spider. In *Function Organization of the Compound Eye*. C. G. Bernhard, editor. Pergamon Press, Oxford. 309.

- DEVOE, R. D. 1967. Nonlinear transient responses from light-adapted wolf spider eyes to changes in background illumination. *J. Gen. Physiol.* **50**:1961.
- DEVOE, R. D., and J. E. ZVARGULIS. 1967. Spectral sensitivities of vision in wolf spiders and jumping spiders. *Fed. Proc.* **26**:655.
- DOWLING, J. E. 1963. Neural and photochemical mechanisms of visual adaptation in the rat. *J. Gen. Physiol.* **46**:1287.
- EKELÖF, S., and G. KIHLEBERG. 1954. Theory of the thermistor as an electric circuit element. A study of thermistor circuits. I. *Trans. Chalmers Univ. Technol., Gothenburg. No. 142.*
- FUORTES, M. G. H. 1959. Initiation of impulses in visual cells of *Limulus*. *J. Physiol., (London)*. **148**:14.
- FUORTES, M. G. H., and A. L. HODGKIN. 1964. Changes in time scale and sensitivity in the ommatidia of *Limulus*. *J. Physiol., (London)*. **172**:239.
- HODGKIN, A. L., and A. F. HUXLEY. 1952. A quantitative description of membrane current and its application to conduction and excitation in nerve. *J. Physiol., (London)*. **117**:500.
- JONES, R. W., D. G. GREEN, and R. B. PINTER. 1962. Mathematical simulation of certain receptor and effector organs. *Fed. Proc.* **21**:97.
- IVES, H. E. 1922. A theory of intermittent vision. *J. Opt. Soc. Am.* **6**:343.
- KELLY, D. H. 1964. Sine waves and flicker fusion. *Doc. Ophthalmol.* **18**:16.
- KIRSCHFELD, K. 1961. Quantitative Beziehungen zwischen Lichtreiz und monophasischem Electroretinogramm bei Rüsselkäfern. *Z. Vergleich. Physiol.* **44**:371.
- KUIPER, J. W., and J. I. LEUTSCHER-HAZELHOFF. 1965. Linear and nonlinear responses from the compound eye of *Calliphora erythrocephala*. *Cold Spring Harbor Symp. Quant. Biol.* **30**:419.
- DELANGÉ, H., DZN. 1961. Eye's response at flicker fusion to square-wave modulation of a test field surrounded by a large steady field of equal mean luminance. *J. Opt. Soc. Am.* **51**:415.
- LEVINSON, J. 1966. One-stage model for visual temporal integration. *J. Opt. Soc. Am.* **56**:95.
- MARIMONT, R. B. 1965. Numerical studies of the Fuortes-Hodgkin *Limulus* model. *J. Physiol., (London)*. **179**:489.
- MARQUARDT, D. W. 1963. An algorithm for least-squares estimation of nonlinear parameters. *J. Soc. Ind. Appl. Math.* **11**:431.
- MAURO, A. 1961. Anomalous impedance, a phenomenological property of time-variant resistance. An analytic review. *Biophys. J.* **1**:353.
- PINTER, R. B. 1966. Sinusoidal and delta function responses of visual cells of the *Limulus* eye. *J. Gen. Physiol.* **49**:565.
- PURPLE, R. L., and F. A. DODGE. 1965. Interaction of excitation and inhibition in the eccentric cell in the eye of *Limulus*. *Cold Spring Harbor Symp. Quant. Biol.* **30**: 529.
- RUSHTON, W. A. H. 1959. A theoretical treatment of Fuortes's observations upon eccentric cell activity in *Limulus*. *J. Physiol., (London)*. **148**:29.
- RUSHTON, W. A. H. 1965. The Ferrier Lecture, 1962. Visual adaptation. *Proc. Roy. Soc. (London), Ser. B.* **162**:20.

- SCHOLES, J. 1965. Discontinuity of the excitation process in locust visual cells. *Cold Spring Harbor Symp. Quant. Biol.* **30**:517.
- TROELSTRA, A. 1964. Non-Linear Systems Analysis in Electro-Retinography. Institute for Perception RVO-TNO, Soesterberg, The Netherlands.
- WALD, G. 1965. Visual excitation and blood clotting. *Science.* **150**:1028.
- WASHIZU, U. 1964. Electrical activity of single retinula cells in the compound eye of the blowfly *Calliphora erythrocephala* Meig. *Comp. Biochem. Physiol.* **12**:369.